# Mechanochemical degradation of perfluorooctane sulfonate using Fe and $\alpha$-$Al_2O_3$: Achieving complete defluoriantion without sulfonate group overreduction

Jin Lin, Xiaoyu Wang, Yushen Kang, Lihua Zhu and Nan Wang*

Key Laboratory of Material Chemistry for Energy Conversion and Storage, Ministry of Education, School of Chemistry and Chemical Engineering, Huazhong University of Science & Technology, Wuhan 430074, China.

*Corresponding author, E-mail: nwang@hust.edu.cn (N. Wang).

## Contents

Number of Pages: 20

Number of Texts: 4

Number of Tables: 3

Number of Figures: 21

## Section S1. Materials and methods

### S1.1 Chemicals

PFOS ($C_8F_{17}SO_3K$, 99% purity) was purchased from J&K Chemical (Beijing, China). Gamma $Al_2O_3$ ($\gamma$-$Al_2O_3$, 99.9%) was purchased from Aladdin Industrial (Shanghai, China). Alpha-$Al_2O_3$ ($\alpha$-$Al_2O_3$, 99.9%) was purchased from Adamas Reagent (Shanghai, China). Boehmite (AlOOH, 99.9%), perfluorooctane ($C_8F_{18}$, 98%) and potassium 1-octanesulfonate ($C_8H_{17}SO_3K$, 98%) were purchased from Macklin Biochemical Technology (Shanghai, China). $K_2Cr_2O_7$ (99%), $Al(OH)_3$ (99%, micron-sized), $MnO_2$ (99%), $La_2O_3$ (99%), ZnO (99%), acetonitrile (MeCN, 99.7%), methanol (MeOH, 99.7%), *t*-butyl alcohol (*t*-BuOH, 99.7%), and 1, 2-dinitrobenzene (DNB, 99.7%) were purchased from Sinopharm Chemical Reagent (Shanghai, China). Iron powder (99.9%, 100−200 mesh), zinc powder (99.9%, 100−200 mesh), aluminite powder (99.9%, 100−200 mesh), HCl (99.7%), NaOH (99.9%), $NH_3 \cdot H_2O$ (99.7%), $CH_3COOH$ (99.7%), and $NH_4COOH$ (99.9%) were purchased from Shanghai Chemical Reagent Supply (China). All chemicals are of analytical reagent grade and used as received without any further purification.

### S1.2 Sample extraction and analysis

The remaining PFOS in the milled samples (20 mg) was extracted by 10 mL aqueous ammonia (0.3 vol%) solution for three times under ultrasound irradiation for 20 min. After centrifuged at 13000 rpm for 8 min, the supernatant solution was filtered through 0.22 μm polyether sulfone (PES) membrane, and the concentration of PFOS in the filtrate was determined on a Thermo Fisher scientific Ultimate 3000 HPLC system using a Symmerrys C18 plus reversed phase column (150 mm × 3.9 mm × 5 μm) and charged aerosol detector (CAD). The inject volume was 40 μL, and column oven temperature was set as 30 °C. A mixture of methanol and $CH_3COOH$-$NH_4COOH$ buffer (5 mM pH = 5.0 ± 0.2) with the volume ratio of 70: 30 was used as the mobile phase and the flow rate was 1.0 mL $min^{-1}$. The nebulizer temperature was 35 °C, and carrier gas pressure was 35 psi. Mass parameters of the 18 PFASs and 9 internal standards (ISs) are shown in Table S2. All other chromatographic conditions were same

as those reported (Zhou et al., 2022). The PFOS calibration curve is shown in **Figure S2.** The recovery yields of PFOS were determined 96.3±6.8% using the standard addition method by spiking PFOS (0.021–0.21 g) into 1.92 g $\alpha$-$Al_2O_3$ and 1.08 g Fe. To identify polar intermediates, the ethanol-extracted solutions were analyzed on ACQUITY UPLC Xevo TQ-S ultra-high performance liquid chromatography tandem mass spectrometer (Waters, America) with the electrospray ionization (ESI) source. A Waters ACQUITY UPLC BEH C18 reversed-phase column (2.1 mm×100 mm×1.7 μm) was employed for chromatographic separation. The mobile phase consisted of methanol solution (mobile phase A) and 2 mmol/L ammonium acetate aqueous solution (mobile phase B). Chromatographic conditions included a column oven temperature of 40 °C, a flow rate of 0.300 mL $min^{-1}$, and an injection volume of 2.0 μL. Gradient elution was utilized with the following program: initial hold at 35% A from 0 to 0.3 min; linear increase to 100% A from 0.3 to 9.0 min; isocratic hold at 100% A from 9.0 to 12.0 min; rapid decrease to 35% A from 12.0 to 12.1 min; and final re-equilibration at 35% A from 12.1 to 17.0 min. Instrument parameters and labelled internal standards used for PFASs quantification by target LC-MS/MS are described in **Table S2**. To identify volatilized organic intermediates, both products in the reactor and gaseous products in the head space of the reactor were collected by using acetone as a solvent. The extract was filtered through a 0.22 μm membrane and then directly analyzed by GC-MS under the same conditions reported in our previous work (Zhou et al., 2022).

$F^-$ produced during the MC defluorination of PFOS was extracted with aqueous NaOH solution (10 mol $L^{-1}$): 20 mg milled sample and 1 mL aqueous NaOH solution was added in a polytetrafluoroethylene (PTFE) sealed jar and heated at 180 °C for 20 min. After the centrifugation to remove the solid, the supernatant was mixed with 10 mL total ionic strength adjustment buffer (TISAB) and 0.75 mL HCl (12 mol $L^{-1}$), followed by diluting with water to 50 mL with pH of 6. The solution was then transferred into a 100 mL PTFE beaker which was immersed in a water bath at 25 °C under stirring and measured with $F^-$-selective electrode (PF-1, Shanghai Electrical Science Instrument,

China). Initial extraction recovery of $F^-$ was determined using its calibration curve of standard solutions (Curve (a) in **Figure S3**) which showed recovery yields of 76.2±2.4% for $F^-$. To improve quantification accuracy, the calibration curve of $F^-$ were subsequently established through quantitatively spiking NaF (0.028–0.280 g) into 3.00 g milling reagents, followed by identical ball milling, extraction and analytical procedures. The resulting calibration curve of $F^-$ is shown as curve (b) in **Figure S3**. Recovery tests using curve (b) demonstrated $F^-$ recovery yields of 97.8±0.9% and thus the calibration curve (b) was adopted for quantitative determination of defluorination efficiencies. To determine the potential generation of $SO_3^{2-}$ and/or $SO_4^{2-}$, 100 mg of the milled samples was extracted with ultrapure water, vortexed for 1 min, sonicated for 15 min and then diluted to a final volume of 10 mL. The extract was detected using a 925 CN ion chromatograph (Metrohm, Switzerland) equipped with a conductivity detector. Separation was performed on a Metrosep A Supp 4-250/4.0 column (4.0 mm × 250 mm, 9 μm) with an eluent consisting of 1.7 mmol $L^{-1}$ $NaHCO_3$ and $Na_2CO_3$ in a 1: 20 (v/v) acetone-water mixture, at a flow rate of 1.0 mL/min.

**S1.3 Characterizations of ball milled samples**

The morphology of milling reagents before and after MC reactions was characterized on a Technai G2 F30 (FEI, America) transmission electron microscopy (TEM). Surface areas and pore volumes of samples were determined from $N_2$ adsorption/desorption isotherms acquired at 100 °C on an automatic ASAP2420-4MP apparatus (Micromeritics, America). X-ray diffraction (XRD) was conducted on a Smart-Lab diffractometer (Rigaku, Japan) with Cu Kα radiation at a speed of 10° $min^{-1}$ and $2\theta$ range of 20 – 80 °. X-ray photoelectron spectra (XPS) were measured on an ESCALAB 250XI spectrometer (Thermo Scientific, America) with Al Kα radiation as the exciting source. Fourier transform infrared (FT-IR) spectra were recorded on Vertex70 spectrometer (Bruker, Germany) by using KBr disk mode with sweeping from 400 to 4000 $cm^{-1}$. Raman spectra were recorded on an inVia Reflex Raman spectrometer (Renishaw, England) with 532 nm laser excitation. Total carbon (TC) content of solid samples was determined using an Multi N/C 3100 analyzer (Shimadzu, Japan). Samples underwent

catalytic combustion at 1000 °C under oxygen carrier gas (200 mL $min^{-1}$) with evolved $CO_2$ quantified by an infrared detector. $CaCO_3$ as a standard was pre-treated at 290 °C for 1 h. After cooling to room temperature at a desiccator, known quantities of $CaCO_3$ (24.6–103.9 mg) were determined to establish a TC calibration curve (**Figure S4**). For sample analysis, 50 mg non-milled or milled samples were collected from the mill jar and then analyzed under identical instrumental conditions.

**S1.4** MC reduction of $Cr_2O_7^{2-}$ using different milling reagents and analysis

$K_2Cr_2O_7$ as a probe was used to evaluate the reduction ability of milling reagents such as $\alpha$-$Al_2O_3$ and/or Fe under ball milling (eq. S1). At a given interval, the milled sample (20 mg) were taken out and extracted with 10 mL NaOH solution (pH 11.0). After the centrifugation and filtration, the pH of extraction solution was adjusted with HCl to pH 2, and the concentration of Cr(VI) was detected by measuring the absorbance at 350 nm on a Cary 60 UV-vis spectrophotometer (Agilent, America).

$$K_2Cr_2O_7 + 6e^- + 4H_2O \xrightarrow{\text{ball milling}} Cr_2O_3 + 2KOH + 6OH^- \qquad (S1)$$

**Table S1** Redox potentials (*E*) of PFOS and the related redox pairs.

| Redox pair | *E* /V vs. NHE | Ref. |
|---|---|---|
| $F^{\bullet}/F^{-}$ | 3.60 | (Dean) |
| $C_8F_{17}SO_3^{-}/C_8F_{17}SO_3^{\bullet}$ | 3.20 | (Carter and Farrell, 2008) |
| $C_8F_{17}SO_3^{-}/C_8F_{17}SO_3^{\bullet}$ | 3.15 | (Shi et al., 2019) |
| $S/H_2S$ | 0.154 | (Dean, , McGraw-Hill, New York, 1991) |
| $Fe^{2+}/Fe$ | –0.440 | (Dean, , McGraw-Hill, New York, 1991) |
| $SO_3^{2-}/S$ | –0.66 | (Dean, , McGraw-Hill, New York, 1991) |
| $Zn^{2+}/Zn$ | –0.763 | (Dean, , McGraw-Hill, New York, 1991) |
| $Al^{3+}/Al$ | –1.66 | (Dean, , McGraw-Hill, New York, 1991) |
| $C_8F_{18}/C_8F_{17}^{\bullet}$ | –2.60 | (Pud et al., 1995) |

**Table S2.** Instrument parameters and labelled internal standards used for PFASs quantification by target LC-MS/MS.

| Analyte | Precursor ion (m/z) | Product ion (m/z) | Collision voltage /V | Cone voltage /V | ISs |
|---|---|---|---|---|---|
| perfluorobutanoic acid (PFBA) | 212.9 | 168.9*/171.9 | 22 | 8 | $^{13}C_4$-PFBA |
| perfluoropentanoic acid (PFPeA) | 262.9 | 219.0*/69.0 | 24 | 7 | $^{13}C_2$-PFHxA |
| perfluorohexanoic acid (PFHxA) | 312.9 | 269.0*/119.0 | 13 | 8/10 | |
| perfluoroheptanoic acid (PFHpA) | 362.9 | 319.0*/168.9 | 30 | 9/16 | $^{18}O_2$-PFHxS |
| perfluorooctanoic acid (PFOA) | 413.0 | 369.0*/169.0 | 18 | 10/19 | $^{13}C_4$-PFOA |
| perfluorobutanoic sulfonic acid ( PFBS) | 298.9 | 79.9.0*/98.9 | 22 | 24/28 | $^{13}C_2$-PFHxA |
| perfluorohexane sulfonic acid ( PFHxS) | 398.9 | 79.9*/98.9 | 20 | 35/35 | $^{18}O_2$-PFHxS |
| perfluoroheptane sulfonic acid ( PFHpS) | 449.0 | 80.0*/99.0 | 65 | 70/100 | $^{13}C_4$-PFOA |
| Perfluorooctane sulfonic acid ( PFOS) | 499.0 | 99.0*/80.0 | 22 | 40/42 | $^{13}C_4$-PFOS |
| 6: 2 fluorotelomer sulfonic acid (6:2 FTS) | 427.0 | 407.0*/81.0 | 8 | 20/25 | $^{13}C_2$-8:2 FTS |
| $^{13}C_4$-PFBA | 217.0 | 172.0* | 14 | 10 | |
| $^{13}C_2$-PFHxA | 315.0 | 270.0*/119.0 | 14 | 10/20 | |
| $^{13}C_4$-PFOA | 417.0 | 372.0*/169.0 | 14 | 10/18 | |
| $^{18}O_2$-PFHxS | 403.0 | 84.0*/103.0 | 56 | 32/30 | |
| $^{13}C_4$-PFOS | 503.0 | 80.0*/99.0 | 60 | 30/28 | |
| $^{13}C_2$ $^{13}C_2$-8:2 FTS | 529.0 | 81.0* | 6 | 28 | |

*The labeled ions were used for quantification, and the non-labeled ions for qualification.

**Table S3**. BET surface area ($S_{BET}$) of $\alpha$-$Al_2O_3$, Fe and $\alpha$-$Al_2O_3$+Fe (mass ratio of 1.8: 1) at MC reaction of 0 and 1 h for the degradation of PFOS.

| Samples | $S_{BET}$ /$m^2$ $g^{-1}$ | |
|---|---|---|
| | $t$ = 0 | $t$ = 1 h |
| $\alpha$-$Al_2O_3$ | 6.41 | 14.36 |
| Fe | 0.57 | 4.19 |
| $\alpha$-$Al_2O_3$+Fe | 3.59 | 11.25 |
| $\sum(0.64S_{BET,\alpha\text{-Al2O3}} + 0.36S_{BET,Fe})$[a] | 4.31 | 10.70 |

[a] In this equation, 0.64 and 0.36 represents the weight fraction of $\alpha$-$Al_2O_3$ and Fe in the mixture, 0.64 $S_{BET,\alpha\text{-Al2O3}}$ and 0.36$S_{BET,Fe}$ are $S_{BET}$ contributed by $\alpha$-$Al_2O_3$ and Fe in the mixture, respectively. At $t$ = 0, $\sum(0.64S_{BET,\alpha\text{-Al2O3}} + 0.36S_{BET,Fe}) > S_{BET,\alpha\text{-Al2O3+Fe}}$, owing to that the surfaces of $\alpha$-$Al_2O_3$ and Fe are covered by each other. At $t$ = 1 h, $\sum(0.64S_{BET,\alpha\text{-Al2O3}} + 0.36S_{BET,Fe}) < S_{BET,\alpha\text{-Al2O3+Fe}}$, indicating that the co-existence of $\alpha$-$Al_2O_3$ suppresses Fe aggregation to increase $S_{BET,Fe}$.

**Table S4**. MC degradation and defluorination of PFOS with different milling reagents.

| Reagents (mass ratio to PFOS) | MC conditions | $Y_{deg}$ /% | $Y_{def}$ /% | Ref. |
|---|---|---|---|---|
| KOH (23: 1) | 275 rpm; 6 h | 99.8 | 92.3 | (Wu et al., 2013) |
| NaOH (23: 1) | 275 rpm; 4 h | 83.7 | 12.6 | |
| CaO (23: 1) | 275 rpm; 4 h | 85.5 | 1.0 | |
| Fe+$SiO_2$ (20.9: 2.1: 1) | 275 rpm; 4 h | 89.1 | 1.5 | |
| $Fe_3O_4$ + Fe (16.9: 5.1: 1) | 600 rpm; 4 h | 98.3 | 95.2 | (Hu et al., 2023) |
| $\alpha$-$Al_2O_3$ + Fe (9.2: 5.1: 1) | 350 rpm; 4 h | 100 | 96.9 | This work |
| $Fe_3O_4$ + Fe (9.2: 5.1: 1) | 350 rpm; 14 h | 100 | 97.0 | |
| KOH (14: 1) | 350 rpm; 26 h | 96.4 | 86.5 | |
| $\gamma$-$Al_2O_3$+$K_2S_2O_8$ | 350 rpm; 26 h | 61.8 | 13.9 | |

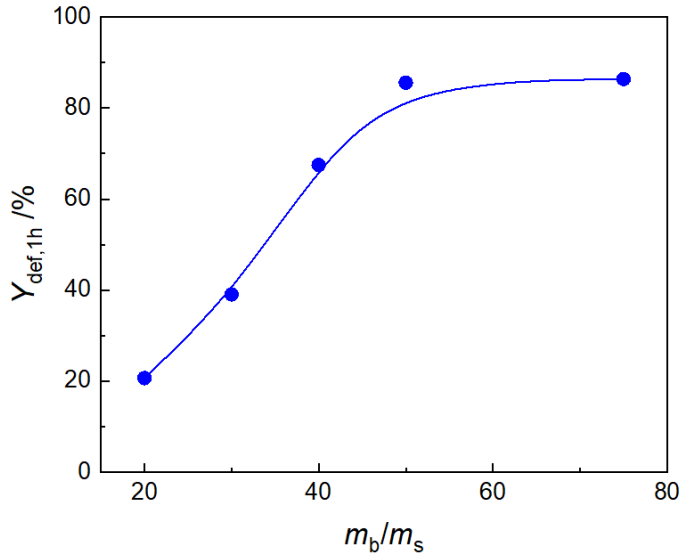


**Figure S1.** Effect of the mass ratio of ball to total reagents ($m_b/m_s$) on defluorination efficiency of PFOS ($Y_{def,\ 1h}$) by 1-h MC treatments using the mixture of $\alpha$-$Al_2O_3$ and Fe.

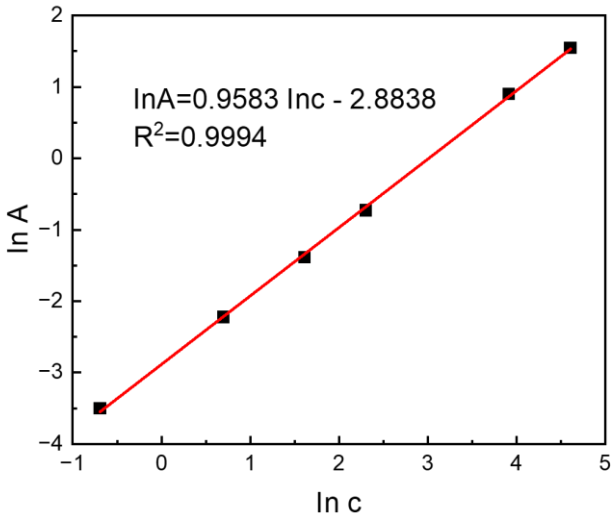


**Figure S2.** Calibration curves of PFOS using HPLC-CAD analysis.

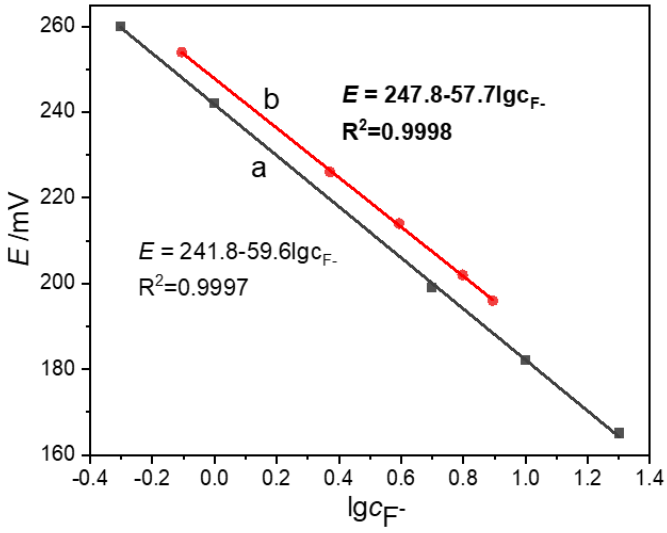


**Figure S3.** Calibration curves of $F^-$ by IC measurements using standard solutions of NaF (a) and extraction solutions (b) from NaF mixed with $\alpha$-$Al_2O_3$ and Fe, subjected to identical ball milling, extraction, and analytical procedures. Recovery tests demonstrated $F^-$ recovery yields of 76.2±2.4% using calibration curve (a) and 97.8±0.9% using calibration curve (b). Given the higher accuracy of curve (b), it was adopted for quantitative determination of defluorination efficiencies.

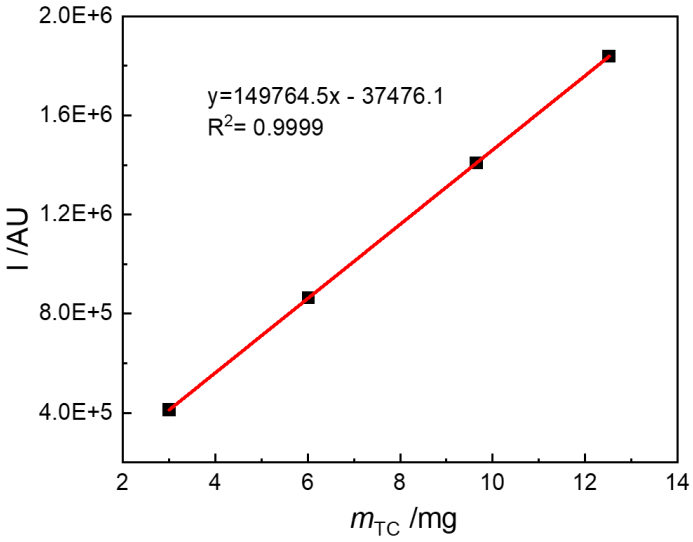


**Figure S4.** Calibration curves of total carbon (TC) content ($m_{TC}$) with $CaCO_3$ as a standard.

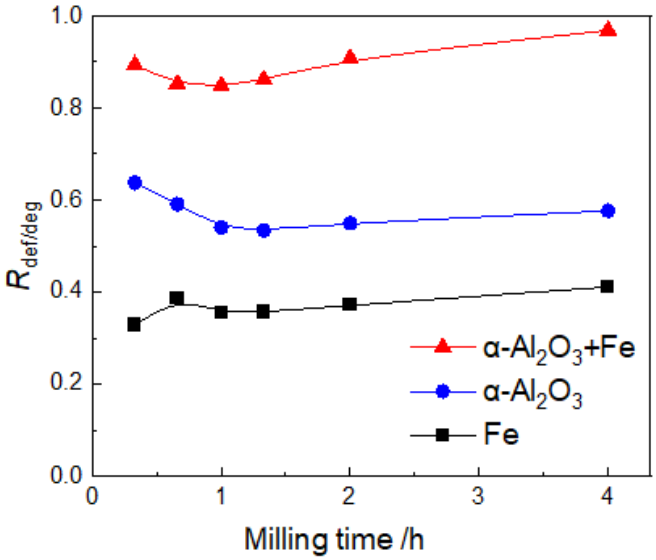


**Figure S5.** Ratio of $Y_{def}$ to $Y_{deg}$ ($R_{def/deg}$) of PFOS with the MC treatment using $\alpha$-$Al_2O_3$, Fe, and $\alpha$-$Al_2O_3$+Fe.

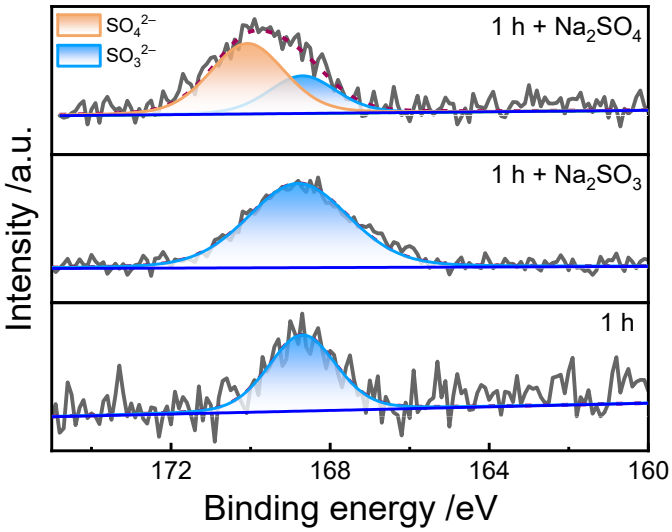


**Figure S6.** High-resolution XPS spectra of S 2p for $\alpha$-$Al_2O_3$+Fe+PFOS at MC reaction for 1 h and its mixture with $Na_2SO_3$ or $Na_2SO_4$ at the molar ratio of 1: 2.

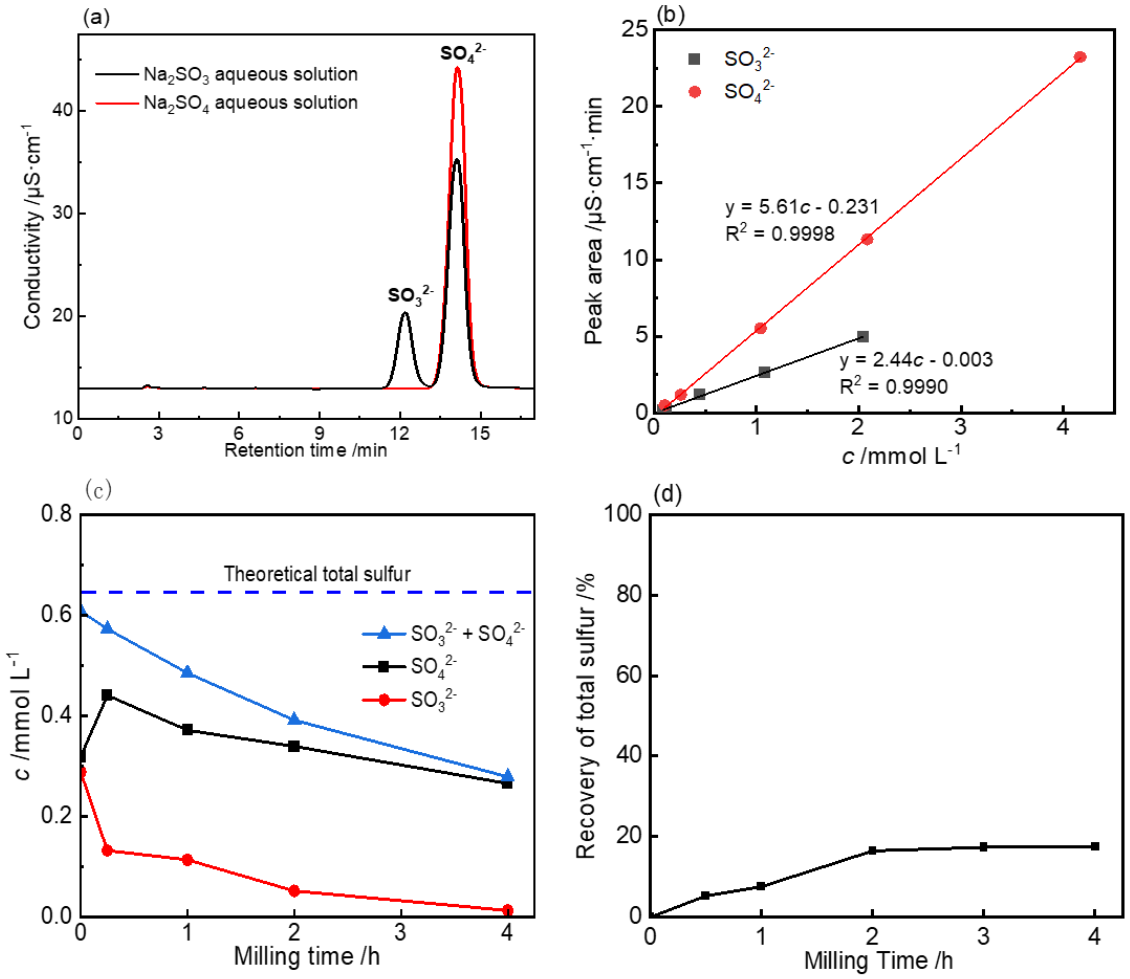


**Figure S7.** (a) Ion Chromatogram of an aqueous solution obtained from dissolving 55 mg of sodium sulfate or 63 mg of sodium sulfite (equivalent to 40 mg of $SO_4^{2-}$ or $SO_3^{2-}$) in 10 mL of ultrapure water followed by 5 min sonification. (b) Calibration curves of $SO_3^{2-}$ (a) and $SO_4^{2-}$ (b) detected by IC measurements. (c) Changes of $SO_3^{2-}$, $SO_4^{2-}$ and their total amount in the aqueous extract of a mixture of $NaSO_3$ (49.1 mg), $\alpha$-$Al_2O_3$ (1.92 g) and Fe (1.08 g) before and after ball milling. (d) Recovery of $SO_3^{2-}$ and $SO_4^{2-}$ (i.e., total dissolved sulfur) obtained from the mixture of PFOS, $\alpha$-$Al_2O_3$ and Fe before and after ball milling. As shown in Figure a, significant conversion of $SO_3^{2-}$ to $SO_4^{2-}$ (59.2%) occurred during solution preparation. In Figure b, the concentration of $SO_3^{2-}$ in standard solutions was corrected by accounting for its conversion to $SO_4^{2-}$ (as quantified by IC). Figure (c) indicates unquantified losses of both $SO_3^{2-}$ and $SO_4^{2-}$ during ball milling.

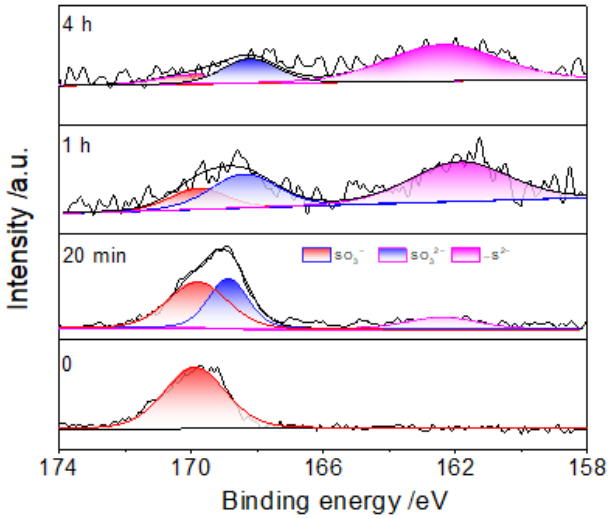


**Figure S8.** High-resolution XPS spectra of S 2p for the mixture of PFOS, $\alpha$-$Al_2O_3$ and Zn at MC reaction of 0 and *t*.

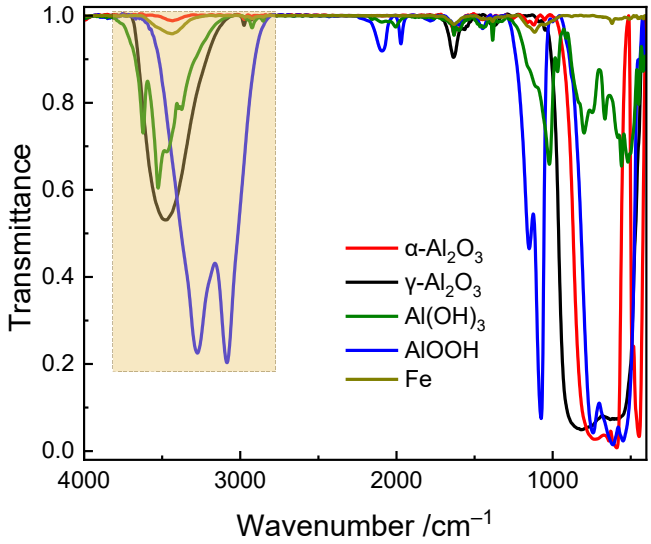


**Figure S9.** FT-IR spectra of $\alpha$-$Al_2O_3$, $\gamma$-$Al_2O_3$, $Al(OH)_3$ and AlOOH, respectively.

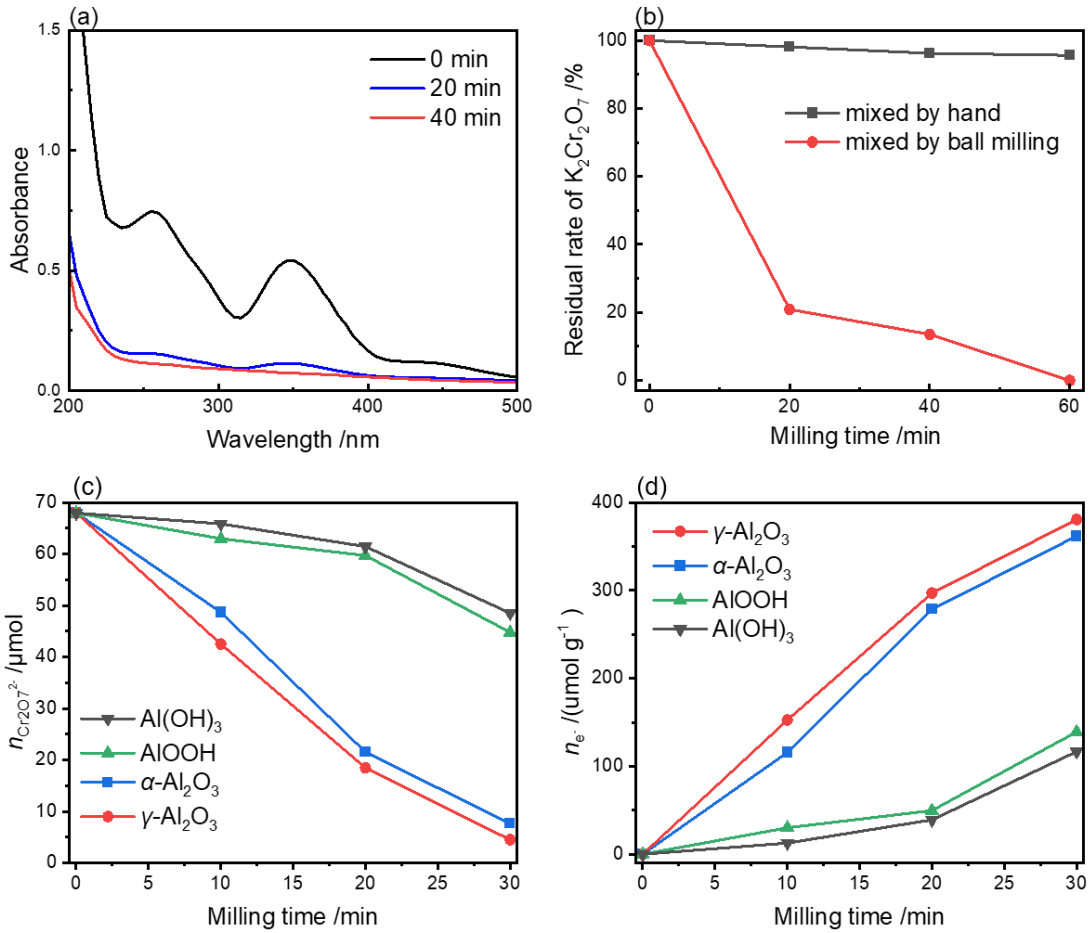


**Figure S10.** (a) UV-Vis absorption spectra of aqueous solution extracted from the mixture of $\alpha$-$Al_2O_3$ $K_2Cr_2O_7$ at different ball milling time. (b) Time profiles for reduction of $K_2Cr_2O_7$ using $\alpha$-$Al_2O_3$ under manual grinding and ball milling. Time profiles for MC reduction of $K_2Cr_2O_7$ (c) and calculated *in-situ* generated electrons ($n_{e^-} = 6\Delta n_{Cr_2O_7^{2-},t} = 6(n_{Cr_2O_7^{2-},0} - n_{Cr_2O_7^{2-},t})$) on per gram milling agents (d) using $\alpha$-$Al_2O_3$, $\gamma$-$Al_2O_3$, $Al(OH)_3$ and AlOOH, respectively, under ball milling.

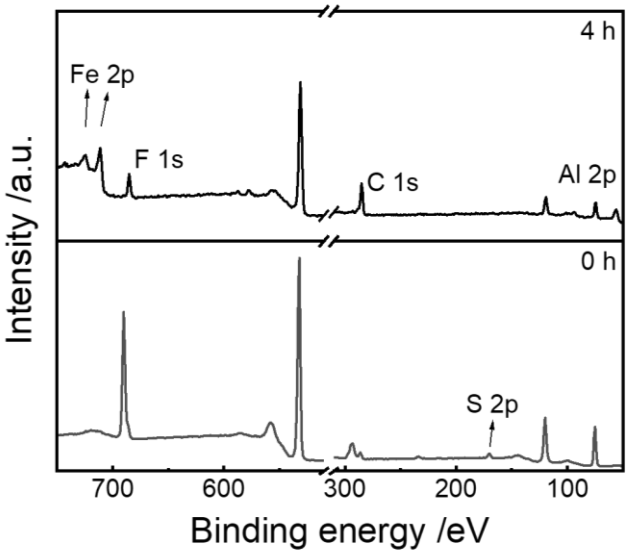


**Figure S11.** Full XPS spectra of C 1s, F 1s, S 2p, Al 2p, and Fe 2p for the mixture of PFOS, $\alpha$-$Al_2O_3$ and Fe at MC reaction of 0 and 4 h.

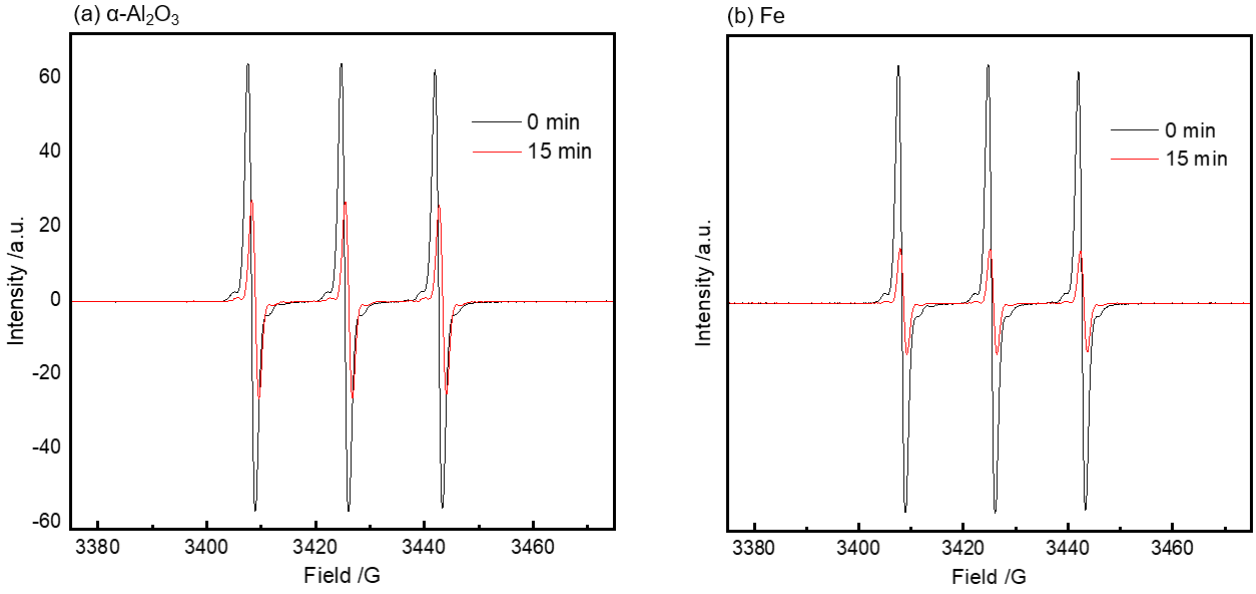


**Figure S12.** ESR spectra obtained from samples of TEMPO comilled with $\alpha$-$Al_2O_3$ (a) or Fe (b).

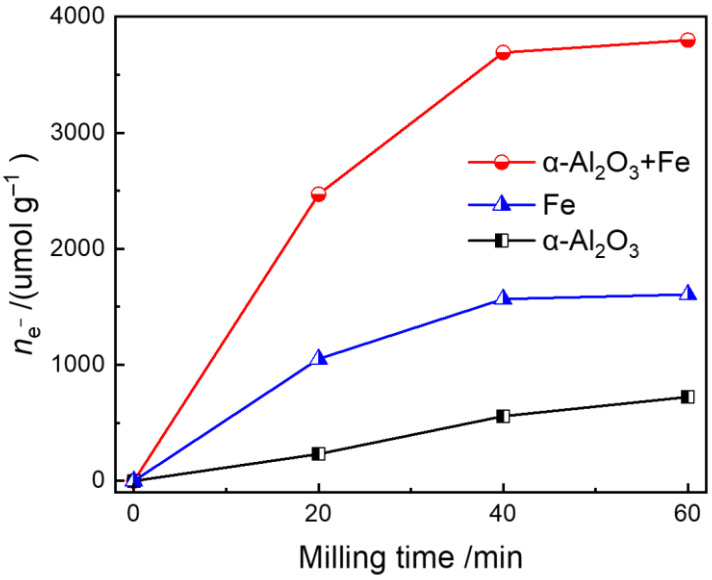


**Figure S13.** Amount of generated electrons calculated from $Cr_2O_7^{2-}$ decay ($n_{e^-} = 6\Delta n_{Cr_2O_7^{2-},t}$)) using $\alpha$-$Al_2O_3$, Fe and $\alpha$-$Al_2O_3$+Fe.

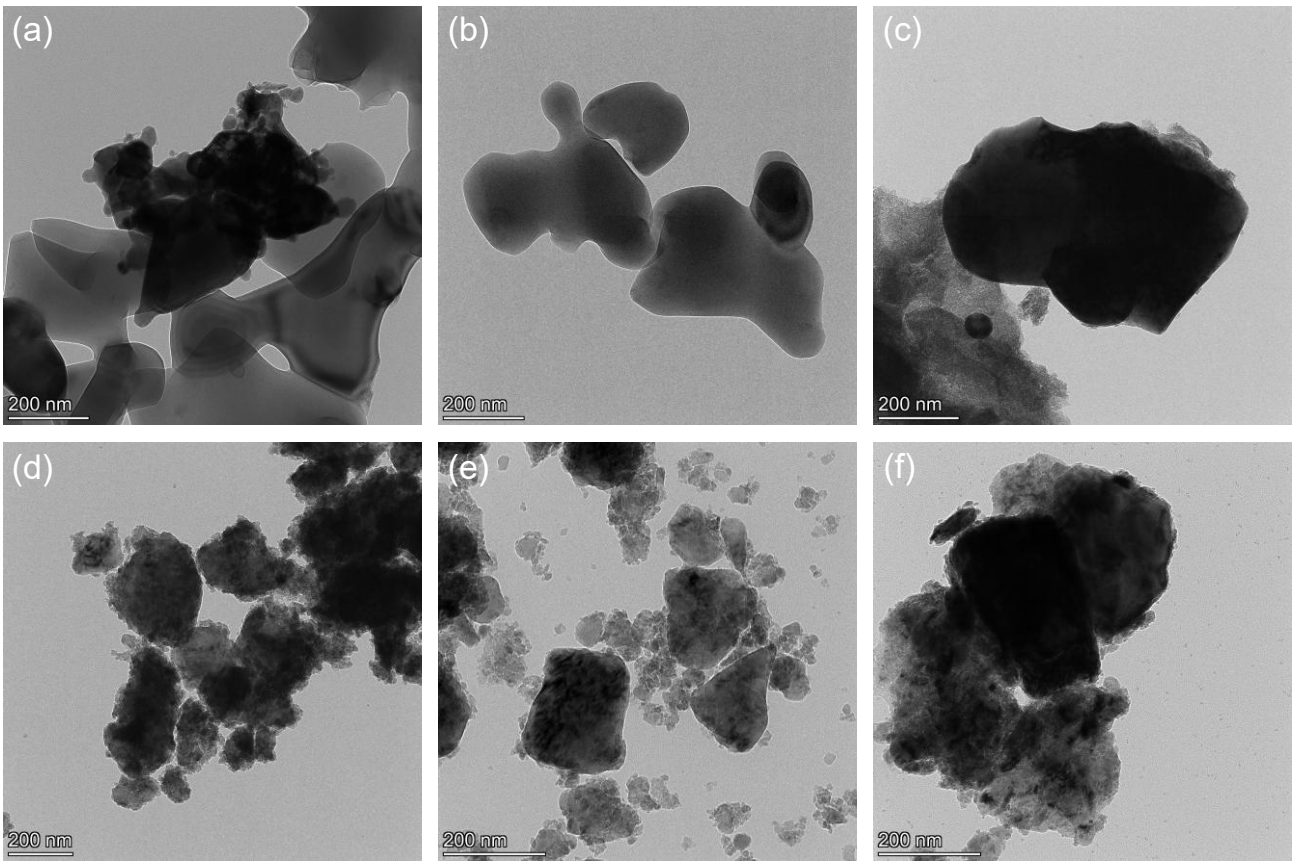


**Figure S14.** TEM images of PFOS+$\alpha$-$Al_2O_3$+Fe (a, d), PFOS+$\alpha$-$Al_2O_3$ (b, e) and PFOS+Fe (c,f) before (a-c) and after the MC reaction for 1 h (d-f).

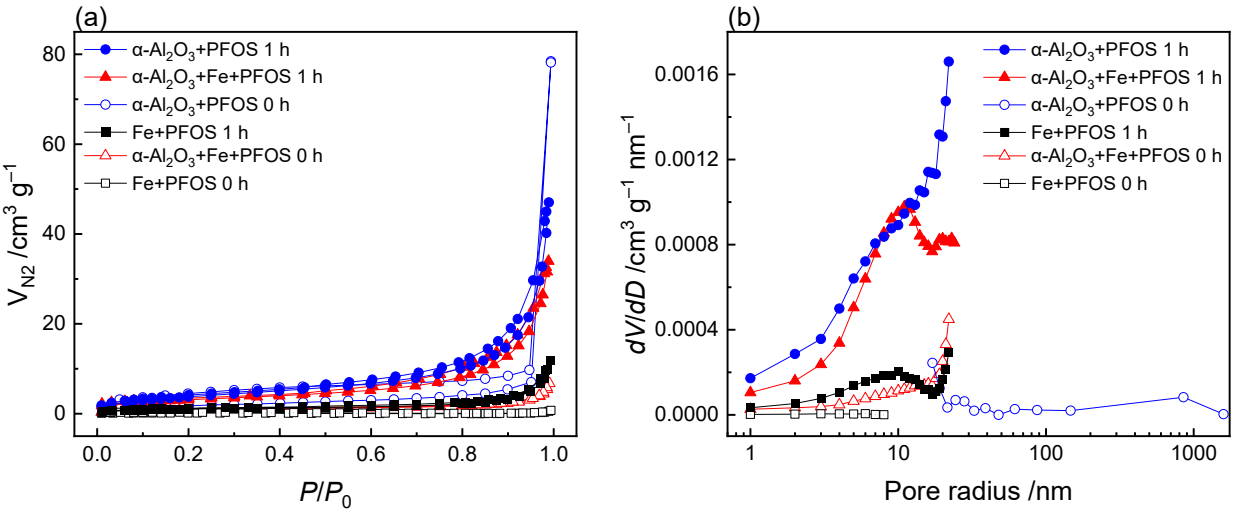


**Figure S15.** $N_2$ adsorption-desorption isotherms (a) and pore size distribution (b) of the mixture of PFOS, $\alpha$-$Al_2O_3$ and/or Fe at the MC reaction of 0 min and 1 h.

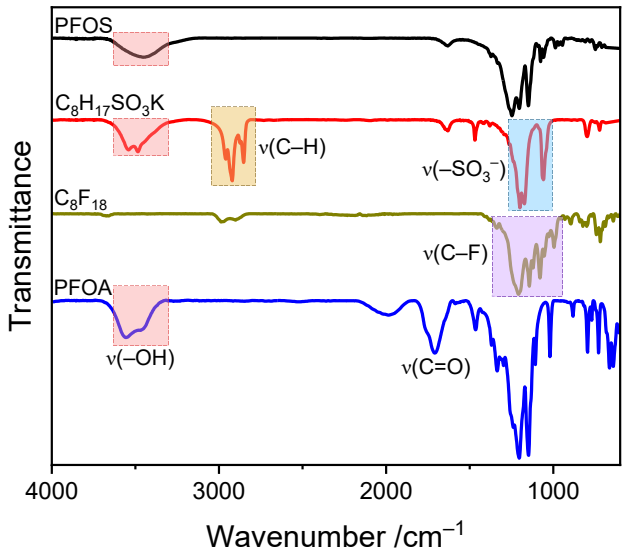


**Figure S16.** FT-IR spectra of PFOS, PFOA, potassium 1-octanesulfonate ($C_8H_{17}SO_3K$) and perfluorooctane ($C_8F_{18}$).

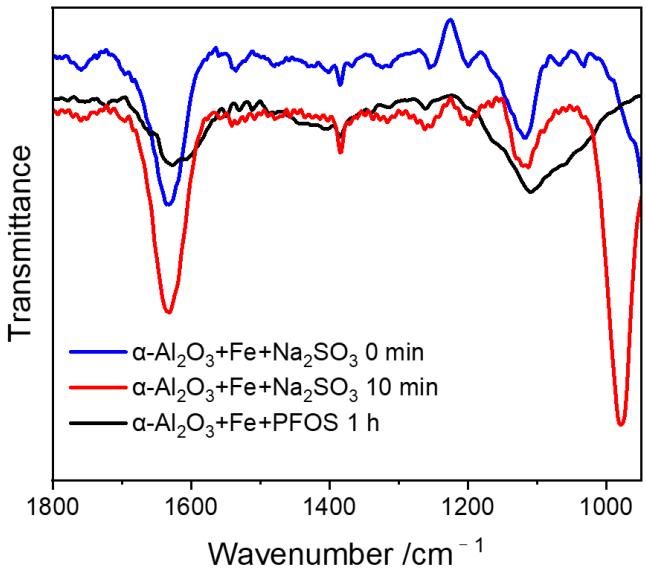


**Figure S17.** FT-IR spectra of PFOS+$\alpha$-$Al_2O_3$+Fe at MC reaction of 1 h and $Na_2SO_3$+$\alpha$-$Al_2O_3$+Fe before and after the MC reaction of 10 min. The molar content of loaded $Na_2SO_3$ is the same as that of PFOS in PFOS+$\alpha$-$Al_2O_3$+Fe.

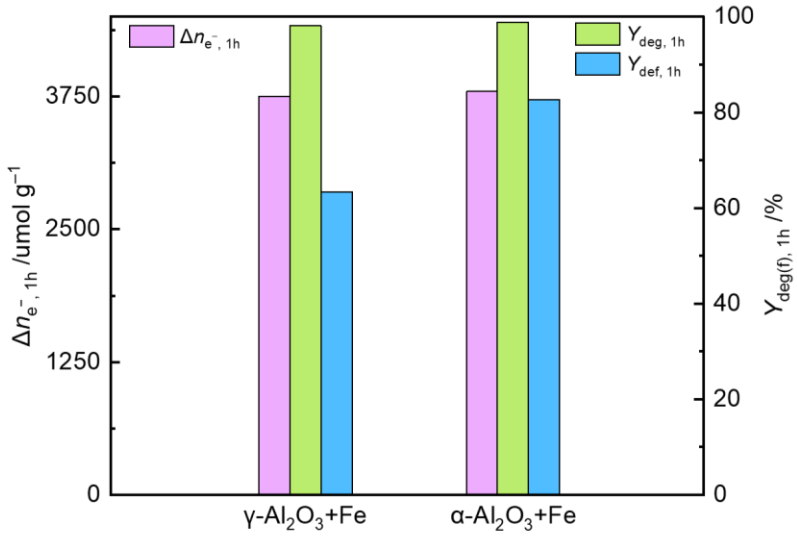


**Figure S18.** Amount of generated electrons ($n_{e^-,1h}$) calculated from $Cr_2O_7^{2-}$ decay and $Y_{def,1h}$ of PFOS using $\gamma$-$Al_2O_3$+Fe and $\alpha$-$Al_2O_3$+Fe at 1-h milling.

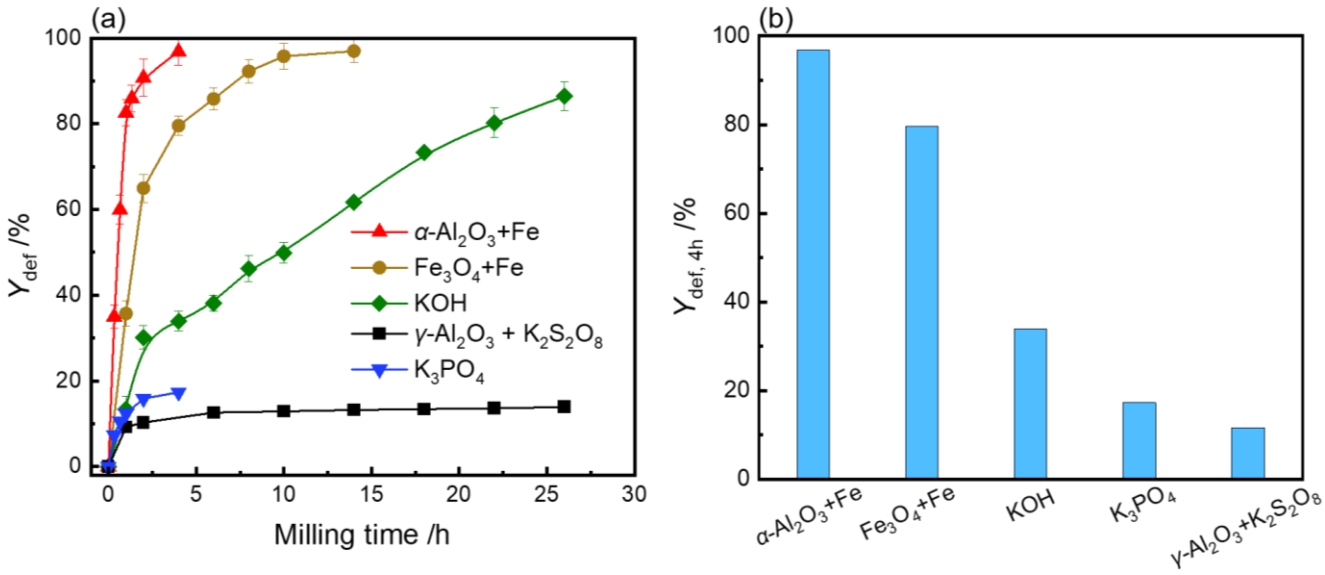


**Figure S19.** $Y_{def}$ (a) and $Y_{def,4h}$ (b) of PFOS with the MC treatment using $\alpha$-$Al_2O_3$+Fe and previous reported reagents including $Fe_3O_4$+Fe, KOH, $K_3PO_4$ and $\gamma$-$Al_2O_3$+$K_2S_2O_8$ at a rotation speed of 350 rpm and the mass ratio of ball to total reagents of 50: 1.

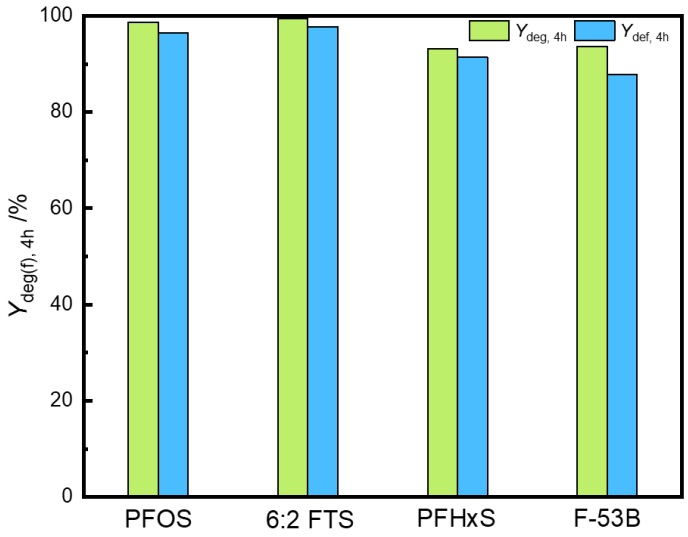


**Figure S20.** $Y_{deg,4h}$ and $Y_{def,4h}$ of PFOS alternatives (F-53B, 6:2 FTS, PFHxS) with $\alpha$-$Al_2O_3$ and Fe at a rotation speed of 350 rpm and the mass ratio of ball to total reagents of 50: 1.

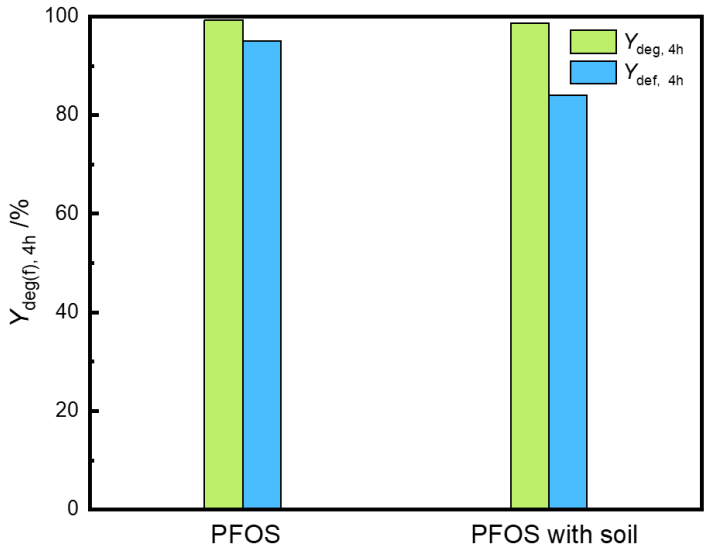


**Figure S21.** $Y_{deg}$ and $Y_{def}$ of PFOS and itself in soil (1.0 g, 190 mg PFOS) with $\alpha$-$Al_2O_3$ and Fe (initial: 1.28 g $\alpha$-$Al_2O_3$ and 0.72 g Fe; supplemental additions at 1 h/2 h: 0.32 g/0.18 g) at a rotation speed of 350 rpm and the mass ratio of ball to total reagents of 50: 1.

**References**

Carter E K, Farrell J (2008). Oxidative destruction of perfluorooctane sulfonate using boron-doped diamond film electrodes. Environmental Science & Technology, 42: 6111–6115

Dean J A (, McGraw-Hill, New York, 1991). Lange's Handbook of Chemistry.

Hu J, Qiu Y, Gu B, Yao N, Lou Z, Cheng Z, Zhang X, Yu J (2023). Enhancement mechanism of magnetite on the ball-milling destruction of perfluorooctane sulfonate by iron. Environmental Pollution, 319: 121014

Pud A A, Shapoval G S, Kukhar V P, Mikulina O E, Gervits L L (1995). Electrochemical reduction of some saturated and unsaturated perfluorocarbons. Electrochimica Acta, 40(9): 1157–1164

Shi H, Wang Y, Li C, Pierce R, Gao S, Huang Q (2019). Degradation of perfluorooctanesulfonate by reactive electrochemical membrane composed of magneli phase titanium suboxide. Environmental Science & Technology, 53(24): 14528–14537

Wu X, Zhang Y, Dou X, Zhao B, Yang M (2013). Fluoride adsorption on an Fe–Al–Ce trimetal hydrous

oxide: Characterization of adsorption sites and adsorbed fluorine complex species. Chemical Engineering Journal, 223: 364–370

Zhou Y, Lv H, Lin J, Lv T, Wang N, Tang H, Zhu L (2022). Complete mechanochemical defluorination of perfluorooctanoic acid using $Al_2O_3$ and Al powders through matching electron-mediated reduction with decarboxylation. Chemosphere, 307: 135872